Chapter 3: Genetic diversities, demographic bottlenecks and coalescence times in a marine metapopulation.

Publication: Bay LK Crozier RH and Caley MJ (In Review) Genetic diversities, demographic bottlenecks and coalescence times in a marine metapopulation. Journal of Evolutionary Biology

Abstract

Metapopulation dynamics are often invoked to explain the complex genetic structure and the evolution of distributional borders of species living in naturally fragmented ecosystems. The habitats of coral reef fishes are highly fragmented, but the evolution of their spatial genetic structure has rarely been examined in a metapopulation context. Here I use a mtDNA sequence marker (control region, n = 296) and three microsatellite loci (n = 316) to examine the evolution of spatial genetic structure in an abundant species of coral reef fish with direct development (*Acanthochromis polyacanthus*). I examine patterns of genetic diversity, historical demography, including local population reduction and/or extinctions, and coalescence times among populations and regions of this species on the Great Barrier Reef (GBR), Australia. Genetic diversities, mismatch and coalescence analyses all identified large variation in the demographic histories in this species among populations and regions. Evidence of genetic bottlenecks was detected by mismatch analysis in the majority of populations sampled (mismatch means = 0.7 – 12.3). In most populations, these bottlenecks appeared to be relatively old since genetic diversities (e.g. $h > 0.6$) and coalescence based population growth estimates ($g < 1000$) did not indicate recent genetic bottlenecks. In contrast, three populations displayed low genetic diversities (e.g., $h < 0.6$) and large population growth rates ($g > 1500$) indicating more recent genetic bottlenecks. Reductions in genetic diversities of local populations resulted in overall lower genetic diversity (e.g., $h = 0.83$, $\pi = 0.007$) and a higher regional expansion rate ($g = 1936$) in the southern region located towards a geographic margin of this species. These results suggest that *A. polyacanthus* exists as a metapopulation within regions on the GBR and that local populations experience periodic genetic bottlenecks and/or extinctions. These fluctuations in local populations have the potential to affect the evolution of the metapopulation and geographical range of this species.

Introduction

Metapopulation theory is often invoked to explain the evolution of spatial genetic structure of populations and the geographical limits of species (Lennon et al. 1997; Holt and Keitt 2000). Many models based on spatially structured arrays of ephemeral populations that interact and persist through time via migration, extinction and re-colonization have been developed to describe such systems (Levins 1970; Hanski and Gilpin 1997; Hanski and Simberloff 1997). Models of metapopulations also often incorporate additional detailed information about fluctuations in population size (Lande et al. 1998). Therefore, within metapopulations, broadly defined, local populations may experience fluctuations in size ranging from small and transient changes to local extinction, and such fluctuations should increase towards the distributional margin of species (Lennon et al. 1997; Holt and Keitt 2000; Holt et al. 2005). The effects of these metapopulation dynamics on spatial genetic structure have typically been measured in terms of genetic differentiation among populations, but may also be evident in patterns of genetic diversity within local populations (Pannell and Charlesworth 1999, 2000; Pannell 2003). As such, important information about the role of local extinctions in a metapopulation and its importance in determining the species range may be gained by examining patterns of genetic diversity, demographic history and genetic differentiation in sets of local populations.

In general, metapopulation dynamics should reduce total genetic diversity (π_T) at the level of the metapopulation and genetic diversity within the sub-populations (π_S) making up a metapopulation compared to a panmictic population equal in size to the metapopulation. The relative magnitude of this difference, however, may vary greatly depending on the frequency and intensity of effective population size reductions among the sub-populations, and the mode of subsequent re-colonization and migration (Pannell and Charlesworth 1999 and references therein). For example, reductions in genetic diversities may be large where reductions in effective size of sub-populations is frequent and large, and if re-colonisation obeys a propagule-pool model, where colonisers originate from a single population. Coalescence times within sub-populations are also reduced under this scenario because of genetic bottlenecks associated with propagule colonisation (Pannell and Charlesworth 1999). If sub-populations experience minor fluctuations in population size, or if colonisation obeys a migrant-pool model, where colonisers originate from a range of populations, sub-populations may not

experience genetic bottlenecks and π_S and π_T may not be affected to a measurable extent (Pannell and Charlesworth 1999, 2000; Pannell 2003).

Coral reef fishes generally display high levels of gene flow, low population genetic structure and large effective population sizes (Palumbi 1994). Consequently, many marine fishes are characterised by relatively shallow population genetic structures with coalescence times indicating the presence of genetic bottlenecks often associated with Pleistocene climate variation (reviewed by Grant and Bowen 1998; Fauvelot et al. 2003). With the exception of a single study, information on demographic bottlenecks and their effects on coalescence times in coral reef fishes are restricted to interspecific comparisons (e.g., Dudgeon et al. 2000; Fauvelot et al. 2003; but see van Herwerden and Doherty 2006). Consequently, we do not have a good understanding of metapopulation dynamics in coral reef fishes.

Coral reef fish species with low dispersal and high genetic structure are the mostly likely to display metapopulation dynamics, and thereby provide opportunities to examine the roles of local extinction and demographic bottlenecks in natural marine systems. One such species is *Acanthochromis polyacanthus.* This species is unusual among coral reef fishes in not having a pelagic larval stage. Instead, it rears its broods within parental territories (Thresher 1985; Kavanagh 2000). Dispersal, which occurs most commonly during the larval phase in coral reef fishes, is restricted in this species and strong genetic and morphological (colouration) differentiation is apparent among reefs and regions (Doherty et al. 1994; Planes et al. 2001; van Herwerden and Doherty 2006; Chapter 2). Populations of *A. polyacanthus* on the Great Barrier Reef (GBR) operate as a metapopulation at intermediate spatial scales (within regions) (Chapter 2). At this spatial scale, populations display high genetic structure in both mtDNA and microsatellite markers. Populations are characterised by low and asymmetric migration and colonisation appears to conform to a propagule-pool model (Chapter 2). Genetic bottlenecks may therefore play an important role through founder effects in producing the strong genetic differentiation observed among reefs in this species (Planes et al. 2001; van Herwerden and Doherty 2006). However, genetic variabilities and demographic histories of this species have only been examined at the regional level. These previous studies suggest that the populations in the southern region of the GBR display lower genetic diversities than in the central and northern regions of the reef when estimated by both allozymes (Doherty et al. 1994) and mtDNA markers (van Herwerden and Doherty 2006) but more ancient population expansion times (van

Herwerden and Doherty 2006). To date, however, analyses of the population genetic structure of this species have been restricted to outer shelf locations on the Great Barrier Reef, offshore reefs, and northern and southern hybrid zones (Planes et al. 2001; van Herwerden and Doherty 2006). Consequently, the genetic structure of the populations of this species remains unexplored throughout large parts of its range on the GBR (but see Chapter 2).

Here I examine patterns of coalescence and demographic bottlenecks within and among regions on the Great Barrier Reef based on both mtDNA and nucDNA markers. I examine the phylogenetic structure of *A. polyacanthus* populations sampled across the continental shelf in three regions on the Great Barrier Reef using a maximum likelihood approach. I then examine the evidence for local population size reductions and/or extinctions by examining genetic diversities among populations, regions and phylogenetic clades. Lastly, I employ two different methodologies, mismatch analysis and a maximum likelihood coalescence approach, to examine the demographic histories of populations and regions. I then interpret these results in the context of metapopulation dynamics at the regional level.

Methods and Materials

Sampling and Laboratory Procedures

A total of 17 populations of *A. polyacanthus* from 3 regions of the GBR, north, central and south, and three individuals from the Solomon Islands were sampled during 2000 – 2003 following the methods outlined in Chapter 2 (Fig. 1). The latitudinal range of *A. polyacanthus* extends from the southern Philippines (10^{o}N) to southern Queensland, Australia (26^{o}S) and the southern region was therefore close to the southern distributional margin of this species. Limited sample sizes were obtained for two other locations (Great Keppel Island n = 10 and Solomon Island n = 3). These two locations were included in the phylogenetic analysis but excluded from all other analyses. DNA was extracted and 356 base pairs of the mtDNA hyper variable control region 1 and three microsatellite loci (Miller-Sims et al. 2005) were amplified, scored and aligned following the methods outlined in Chapter 2.

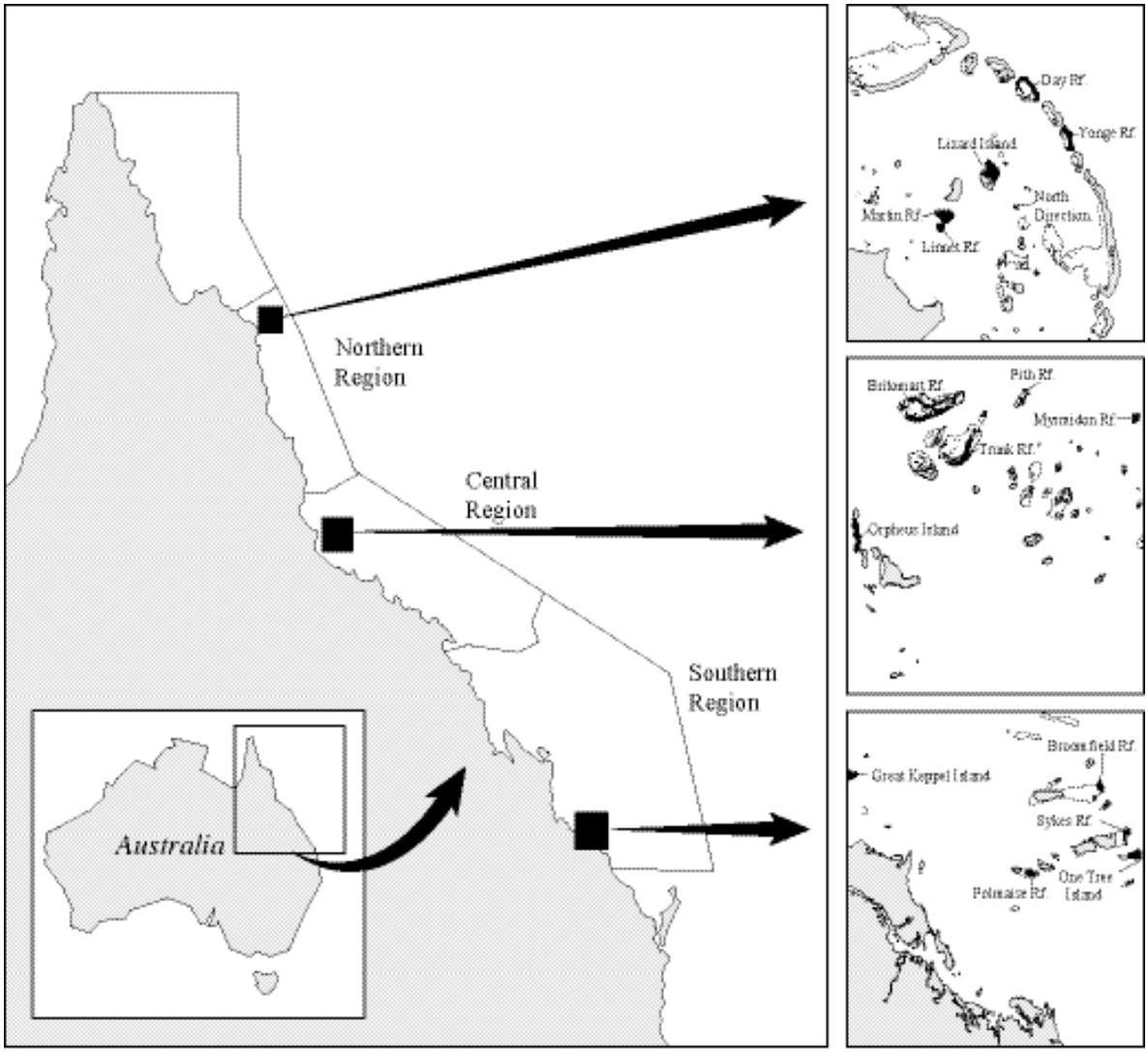

Fig. 1: The sampling locations of *Acanthochromis polyacanthus* on the Great Barrier Reef.

Sequences have been deposited in GenBank under accession numbers DQ199666 – DQ199947, DQ204725 – DQ204734, DQ206818 – DQ206820.

Population genetic investigations commonly use a single mitochondrial marker, which introduces some uncertainty about whether results are gene specific or representative of population level processes (Avise 2000). Therefore, the analysis of the microsatellites here was intended to provide an assessment of population structure independent of the mtDNA. Because of the relatively low number of microsatellite loci screened, interpretations based on these data should be regarded with some caution.

Phylogenetic Analysis

The best model of nucleotide substitution was determined using MrModeltest 2.2 (Nylander 2004) and Paup* 4.0b10 (Swofford 1998). The hierarchical likelihood tests and Akaike Information Criteria agreed that the GTR model with a $\gamma = 0.507$ best fitted the data (-LogLikelihood = 1914.9; AIC = 3847.8). This model and rate heterogeneity estimate was used in the phylogenetic analysis. The phylogenetic structure of *A. polyacanthus* was explored using Bayesian inference implemented in MrBayes 3.0B4 (Huelsenbeck and Ronquist 2001). The analysis was performed using a Markov Chain Monte Carlo search with four chains for one million generations. Trees were sampled every 100 generations and the first 100,000 generations were discarded as burn-in. The tree was rooted by an outgroup consisting of two closely related species, *Amphiprion melanopus* and *A. akindynos*. Credibility values were obtained from a majority rule consensus tree of the last 2000 trees and values greater than 90% are indicated on the major nodes of the tree. For the population level analyses of the ingroup the best model of nucleotide substitution was determined using Modeltest 3.5 (Posada and Crandall 1998) and Paup* 4.0b10 (Swofford 1998). The hierarchical likelihood tests and Akaike Information Criteria agreed that the Tamura and Nei model (Tamura and Nei 1993) with a $\gamma = 0.301$ best fitted the data (-LogLikelihood = 1220.7; AIC =2453.3). This model and rate heterogeneity estimate was used in all population level analyses.

The phylogenetic analysis of the mitochondrial control region sequences identified the presence of three divergent lineages on the GBR and the mitochondrial and nuclear population genetic datasets were categorised on the basis of these. Five groups were obtained of which three groups were based on the three major phylogenetic clades and two groups were based on geographic location within one of the clades (Clade 3). The "South" group contained all Clade 1 fish. The "Clade 2" group contained all northern region fish encompassed in the mtDNA Clade 2. The "Clade 3" group contained all Clade 3 individuals from the northern and central regions. The "Clade 3N" group was a subgroup of Clade 3 and contained all Clade 3 fish from the northern region. The "Central" group was also a subgroup of Clade 3 and contained all the fish from the central region. Because the nucDNA did not display any significant structure based on the mtDNA clade structure (Clade 2 vs. Clade 3N: Pairwise $R_{ST}= 0.003$, $P = 0.35$) the microsatellites were analysed on the basis of geographic location only.

Genetic Diversities

Estimates of mitochondrial haplotype and nucleotide diversity (Tajima 1983, 1993; Nei 1987) and their associated standard deviations were calculated using Arlequin 2.000 (Schneider et al. 2000) for each population and region. Standard deviations were converted to 95% confidence intervals as 95% CI = $\pm$1.96*(SD/$\sqrt{}$ (n)). For each population also, allele frequency and richness and the frequency of private alleles were estimated using Fstat 2.9.3.2 (Goudet 2001), while allelic diversity and heterozygosity were calculated using Arlequin. Mean genetic diversities and 95% confidence intervals were plotted and interpreted as being statistically different when error estimates did not overlap.

Demographic History

A range of analytical techniques are available for reconstructing past demography based on the identity and frequency of genotypes within and among populations (Knowles 2004). Existing techniques employ different methodologies including frequentist, cladistic and Bayesian approaches, but do not always calculate error estimates associated with models and their parameters. (Knowles and Maddison 2002). Because of the potential role of fixed effects in these statistical models, and the frequency with which natural systems may violate their assumptions, these methods often produce historical demographic parameters with large error estimates making conclusions about the demographic histories of populations difficult to draw (Knowles and Maddison 2002). The concurrent application of several of these analytical tools, and careful interpretation of error estimates where they do exist, can ameliorate some of the problems associated with the interpretation of such analyses (Knowles 2004).

Demographic histories were explored by mismatch analysis of mtDNA sequence data using Arlequin and 1000 bootstrap replicates. This analysis compares the distribution of pairwise nucleotide differences to a permuted distribution under the null hypothesis of sudden expansion. The age of population expansion (τ) is also estimated ($\tau = 2\mu t$, where μ = the mutation rate and t = generation time). Mismatch analysis was conducted based on geographical position (reef location and region) and phylogenetic clade membership (Clade 1, 2 and 3 from Fig. 2) independently. Because the mismatch mean of a population is inflated by genetic substructure, the spatial scale at which these comparisons were made was kept constant by analysing northern and central individuals of Clade 3 separately (Clade 3N and Central respectively). The age of population

expansion (τ) values were considered significantly different when their 95% confidence intervals did not overlap.

Demographic bottlenecks in the microsatellites were investigated by examining the conformation to mutation-drift equilibrium (as identified by heterozygote excess) among populations and regions under the Infinite Allele Model (IAM) and the Stepwise Mutation Model (SMM) using one-tailed Wilcoxon tests (1000 bootstrap replicates) implemented in Bottleneck 1.2.02 (Piry et al. 1999).

The exponential population expansion parameter (g) was calculated among locations, regions and clades using a maximum likelihood coalescence approach implemented in FLUCTUATE 1.4 (Kuhner et al. 1998). A search strategy, each 10000 steps long using ten short chains, sampling every 20th step, followed by ten long chains each of 20000 steps sampled every 20th step, gave consistent results among runs and was used in all analyses. Estimates of g and their associated standard deviations were plotted and interpreted as significantly different if these error estimates did not overlap. Allele frequency data cannot presently be used in FLUCTUATE. This analysis was therefore restricted to the mtDNA data. The information obtained from all demographic history analyses were summarised into four demographic history models for interpretative purposes.

Results

Phylogenetic Structure

356 bases of the mtDNA control region I were obtained from 296 individuals sampled from 17 locations. The Bayesian analysis produced a well-resolved tree (-ln likelihood = 2146.39) and the ingroup was monophyletic (Fig. 2). Three clades were well resolved with credibility values greater than 90%. One clade (Clade 1) was further split into two clades of which one was well supported (Clade 1, credibility value = 100%) and the other less well supported (Clade 2, credibility value 72%). Clades 1 and 2 are sister clades to Clade 3 (credibility value = 100%). Clade 1 (credibility value = 100%) is composed of all individuals from the southern region and does not contain individuals from other regions. Clade 2 is comprised of individuals from the northern region with a high proportion of individuals from the two inner shelf (Martin and Linnet) and one midshelf reef (North Direction) (Fig. 2). Clade 3 (credibility value = 95%) is the largest clade in the tree and contains individuals from all reefs from the northern and central regions (although the three primary reefs in Clade 2 (Martin, Linnet, North Direction)

are represented by few individuals) (Fig. 2). Clade 4 (credibility value = 100%) is the most basal clade in the ingroup and the sister clade to Clades 1 - 3. It was exclusively composed of three individuals from the Solomon Islands (Fig. 2).

Fig. 2: Bayesian tree of 100 unique sequences from *A. polyacanthus* and outgroups. Internal branch support estimates greater than 90 are shown.

Patterns of Genetic Diversity

Genetic diversities of both mtDNA and microsatellite markers were generally high and variable among regions (Fig. 3). Haplotype diversities were very high when summed over all populations (total (± 95%CI) = 0.97 (±0.0003)) and high in the northern and central regions (and consequently also high in Clade 3 and its subgroup Clade 3N). Haplotype diversities, however, were significantly lower and much more variable among locations in the southern region and in Clade 2 (Fig. 3a). Nucleotide diversities were generally high (total (± 95%CI) = 6.6% (±0.37)), and highest and most variable, in the northern region. Nucleotide diversities were low in Clade 2 and generally declined toward the south (Fig. 3b). Allelic diversities displayed a very similar pattern to that of the nucleotide diversities: they were generally high (total (± 95%CI) = 1.00 (± 0)), greater in the northern region and declined with increasing latitude (Fig. 3c). Heterozygosities were high (total (± 95%CI) = 0.9 (±0.04)) and did not differ among regions (Fig. 3d).

Genetic diversities varied among reefs (Fig. 4). Each region contained one or two reefs with significantly lower haplotype diversities than the rest (i.e., North = Yonge, Central = Trunk, south = One Tree Island and Sykes) (Fig. 4a). In the southern region, the allelic diversity pattern was opposite to that of the mtDNA (lowest at Polmaise and Broomefield, highest at One Tree Island and Sykes) (Fig. 4c). Heterozygosity estimates were associated with large variances and did not differ among reefs within or among any of the regions (Fig. 4d).

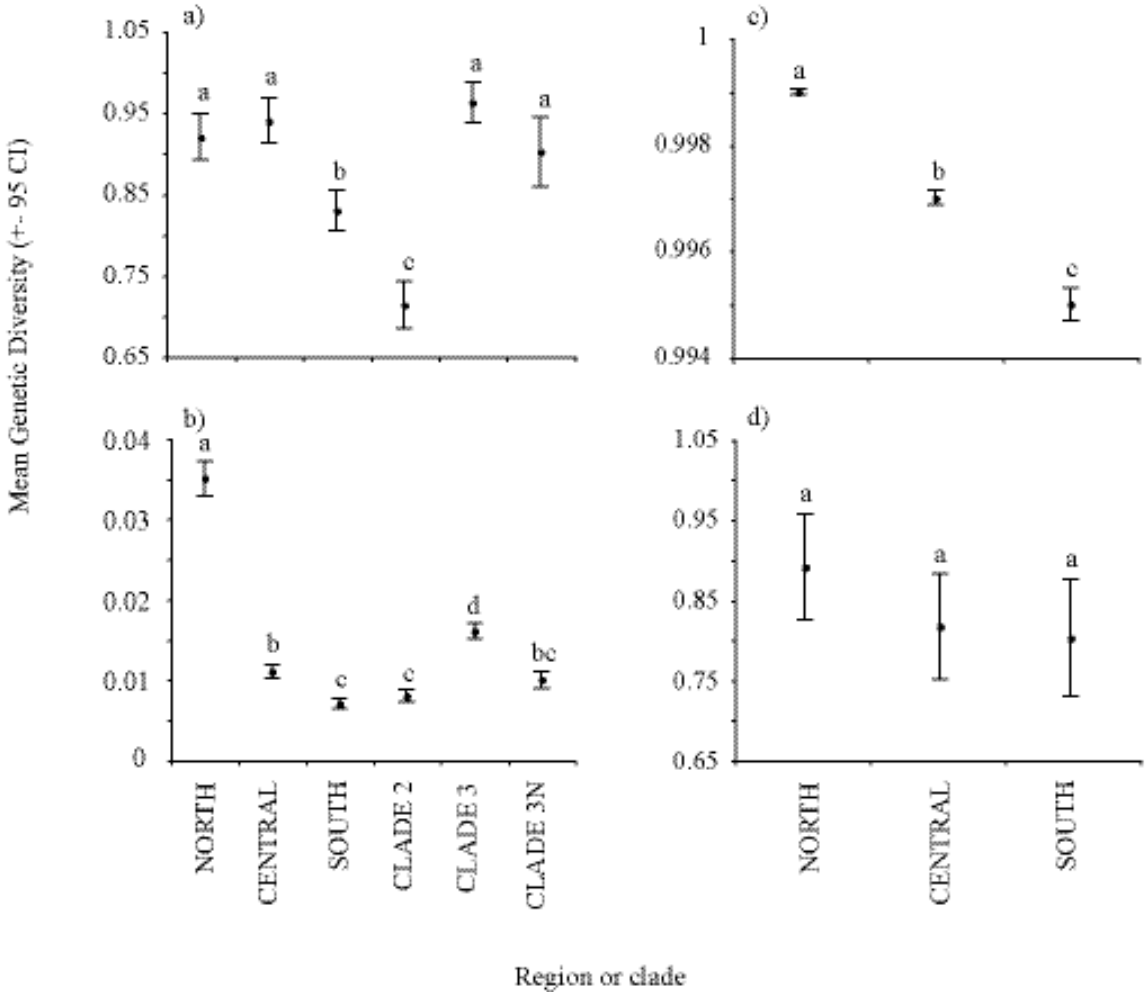

Fig. 3: Genetic diversities among regions and clades. a) Haplotype diversity and b) nucleotide diversity of mtDNA, c) allelic diversity and d) heterozygosity of the microsatellites. Statistical differences have been indicated with letters (shared letter = not significantly different) above means.

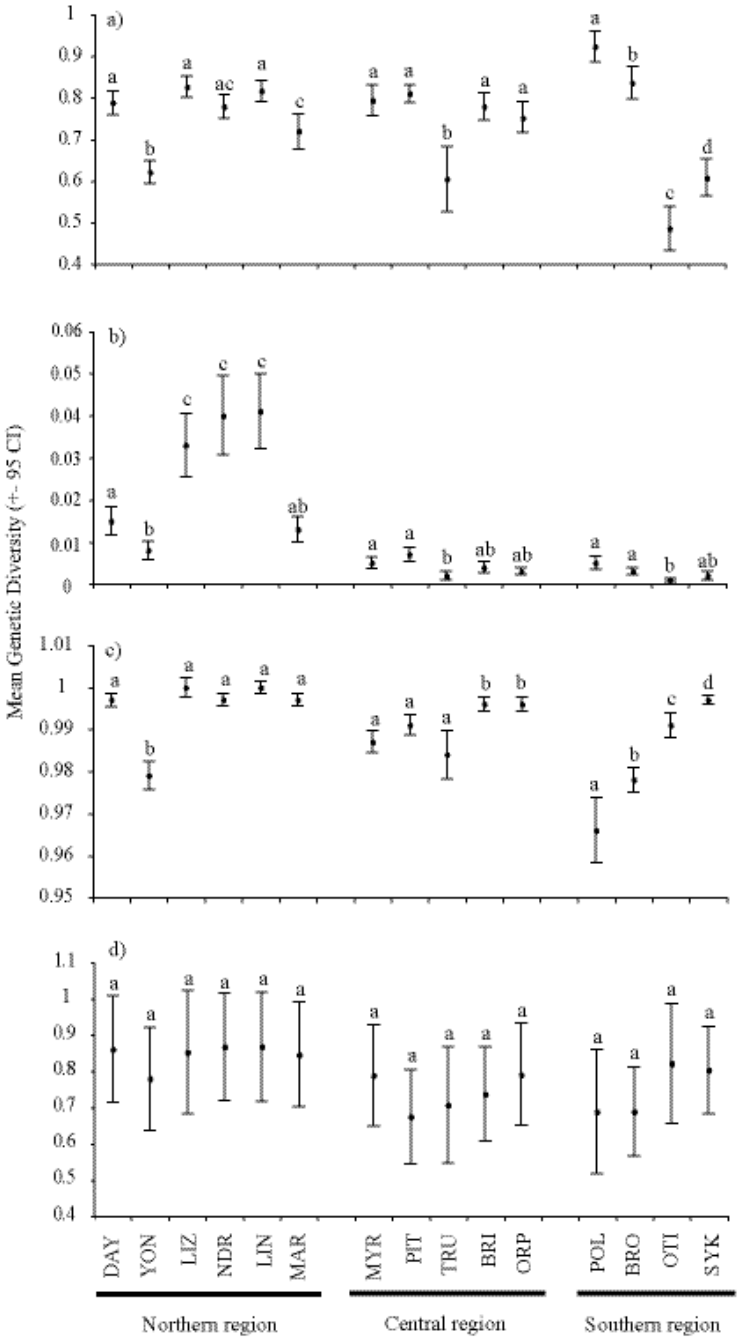

Fig. 4: Genetic diversities among reefs within regions. a) Haplotype diversity and b) nucleotide diversity of mtDNA, c) allelic diversity and d) observed heterozygosity of the microsatellites. Location abbreviations are: BRI = Britomart Reef, BRO = Broomefield Reef, DAY = Day Reef, LIN = Linnet Reef, LIZ = Lizard Island, MAR = Martin Reef, MYR = Myrmidon Reef, NDR = North Direction Island, PIT = Pith Reef, OTI = One Tree Island, ORP = Orpheus Island, POL = Polmaise Reef, SYK = Sykes Reef, TRU = Trunk Reef, YON = Yonge Reef. Statistical differences have been indicated for each region separately with letters (shared letter = not significantly different).

The number of alleles and allele richness were generally high and varied among populations and loci (Table 1). Microsatellite AC 42 had the highest number of alleles (24 at Martin) and highest allele richness (19.34 at Sykes). Microsatellite AC33 displayed the lowest number of alleles (3 at Britomart and Polmaise) and lowest allele richness (2.8 at Trunk). Private alleles were infrequent at most loci and populations, but one allele of microsatellite AC37 was more frequent at Yonge Reef (Table 1).

Historical Demography and Population Expansion

Mismatch analyses indicated that sudden expansion could not be rejected for any region or clade (Table 2). The mean number of pairwise differences ranged from 2.3 in the southern region to 12.3 in the northern one. There was, however, considerable uncertainty associated with the northern estimate (Fig. 5a). The age of population expansion (τ) ranged from 0.7 in Clade 2 (the southern region) to 6.5 in Clade 3. There were no statistically significant differences in this parameter among regions or clades. In the southern region, the lower bound of the 95% confidence interval could not be distinguished from 0 (Fig. 5b). Estimates of population expansion varied greatly among regions and clades (Fig. 5c). Estimates of population expansion were significantly greater in the southern region, intermediate in the central region, and close to 0 in the northern region (Fig. 5c). Population expansion rates were more variable in the two northern clades (Clade 2 and Clade 3N) and were significantly greater in Clade 3N compared to the northern region. Clade 3 was intermediate to the northern and the central regions.

The mismatch analysis indicated that the genetic architectures of all populations except two (i.e., North Direction and Linnet) were consistent with a model of sudden expansion (Table 2). These two populations were characterised by intermediate proportions of individuals contained in Clade 2 and 3, respectively (Fig. 2). The microsatellites did not reveal population bottlenecks under either the IAM or SMM models at any of the reefs (Table 2).

Mismatch distribution means were variable among reefs and ranged from 0.7 (Sykes) to 11.8 (Linnet). Reefs from the northern region that contained 20 – 65 % of individuals contained in Clade 2 had greater mismatch means, and larger uncertainty (Fig. 6a). Mismatch means were lower and more similar among reefs in the central and southern regions. The age of population expansion (τ) followed a similar pattern to that of the mismatch means.

Table 1: Genetic diversity indices from three microsatellite loci among 15 populations of *Acanthochromis polyacanthus* on the Great Barrier Reef including average number of alleles, mean allelic richness per population, number of private alleles and their frequencies, observed and expected heterozygosity.

	Number of alleles			Allelic richness			Private alleles (frequency)			Observed H			Expected H		
Locus	AC33	AC37	AC42	AC33	AC37	AC42	AC33	AC37	AC42	AC33	AC37	AC42	AC33	AC37	AC42
Reef															
Day Reef	7	13	26	5.964	10.22	17.75	0	1 (0.042)	2 (0.042)	0.625	0.708	0.833	0.737	0.845	0.944
Yonge Reef	6	8	11	5.52	6.36	8.65	0	1 (0.159)	0	0.636	0.636	0.636	0.755	0.753	0.777
Lizard Island	10	10	23	8.712	9.27	18.65	0	1 (0.056)	1 (0.028)	0.778	0.778	0.722	0.776	0.764	0.944
North Direction	12	11	20	9.36	8.64	15.01	1 (0.042)	0	1 (0.021)	0.958	0.542	0.625	0.845	0.774	0.928
Linnet Reef	7	15	23	5.762	11.99	17.42	0	1 (0.022)	3 (0.108)	0.739	0.783	0.522	0.713	0.891	0.940
Martin Reef	7	11	24	4.872	9.80	12.17	1 (0.021)	0	2 (0.084)	0.458	0.792	0.792	0.703	0.833	0.944
Myrmidon Reef	6	12	17	3.237	8.15	16.88	0	0	0	0.435	0.826	0.870	0.580	0.870	0.862
Pith Reef	4	11	22	3.853	6.83	16.46	1 (0.024)	0	0	0.286	0.571	0.905	0.323	0.715	0.934
Trunk Reef	4	7	18	2.795	9.67	16.82	1 (0.067)	0	1 (0.033)	0.4	0.333	1.000	0.429	0.700	0.920
Britomart Reef	3	11	23	6.807	8.74	13.93	0	0	2 (0.042)	0.292	0.833	0.917	0.369	0.851	0.943
Orpheus Island	9	11	19	3	7	10	0	0	1 (0.043)	0.217	0.870	0.826	0.553	0.854	0.911
Polmaise Reef	3	7	10	3.336	8.54	7.46	0	0	0	0.154	0.769	0.692	0.500	0.698	0.787
Broomefield Reef	4	10	9	6.133	9.01	16.35	0	0	0	0.042	0.917	0.708	0.376	0.845	0.799
One Tree Island	7	10	20	7.18	7.39	14.42	0	0	4 (0.167)	0.500	0.722	0.833	0.637	0.832	0.926
Sykes Reef	10	10	21	8.333	12.2	19.34	2 (0.048)	0	3 (0.048)	0.290	0.774	0.806	0.674	0.770	0.922

Error estimates from most reefs in all three regions overlapped to a great extent. Greater values with large variances were observed in two northern reefs (North Direction and Linnet), lower and less variable estimates were found in one central location (Trunk) and in two southern locations (One Tree Island and Sykes) (Fig. 6b). The age of population expansion (τ) could not be distinguished from 0 in four locations: Trunk and Orpheus Island in the central region and One Tree Island and Sykes in the southern region. Population expansion rates varied significantly among locations (Fig. 6c). All northern locations displayed negative growth rates close to 0. Reefs in the central region showed both positive and negative growth rates that were all close to 0 except Trunk that displayed a highly positive value. The high mean regional growth rate in the southern region (Fig. 5c) was contributed to by three of the four reefs having growth rates that were greater than all other reefs except one (Trunk in the central region) (Fig. 6c).

Discussion

The analyses of the mtDNA of *A. polyacanthus* indicated a complex phylogenetic structure with evidence of population expansion at most spatial and phylogenetic scales examined. There were substantial differences in the timing of these expansions and the population expansion rates among regions and reefs within regions. These results indicate that local populations of *A. polyacanthus* have experienced periodic reductions in population size, and possibly local extinctions. Taken together these results suggest that the evolution of the spatial dynamics of this species are best interpreted in a metapopulation context.

Population Demography among Regions

Patterns of haplotype, nucleotide and allelic diversity, mismatch analyses and population growth estimates all indicated substantial differences in the demographic histories of *A. polyacanthus* among regions on the GBR (Fig. 3a – c, Fig. 5a - c). The southern region, located close to the species' southern border, was characterised by lower nuclear and mitochondrial genetic diversity and a expansion rate 5 – 10 times greater than the central and northern regions (Fig. 5c).

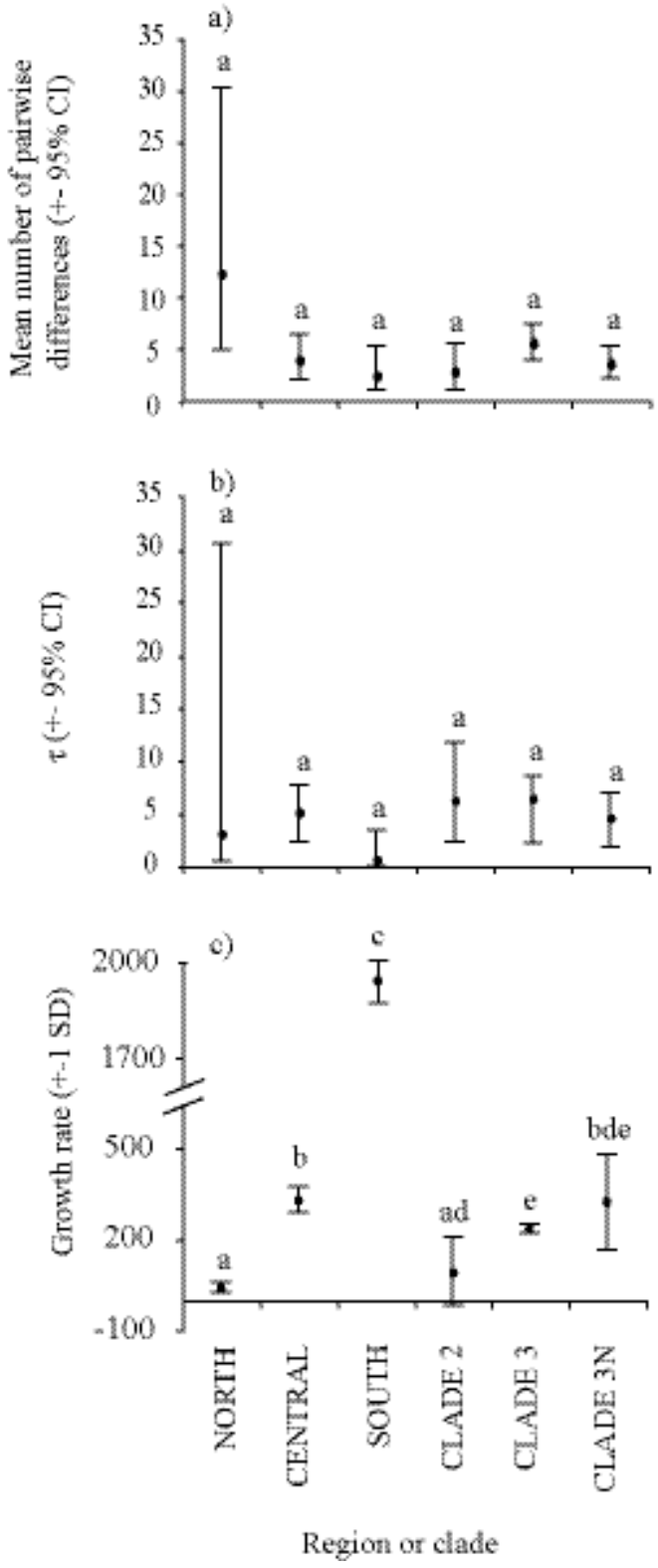

Fig. 5: Mismatch means, expansion parameter (τ) and population expansion rates (*g*) among regions and clades. Statistical differences have been indicated with letters (shared letter = not significantly different) above means.

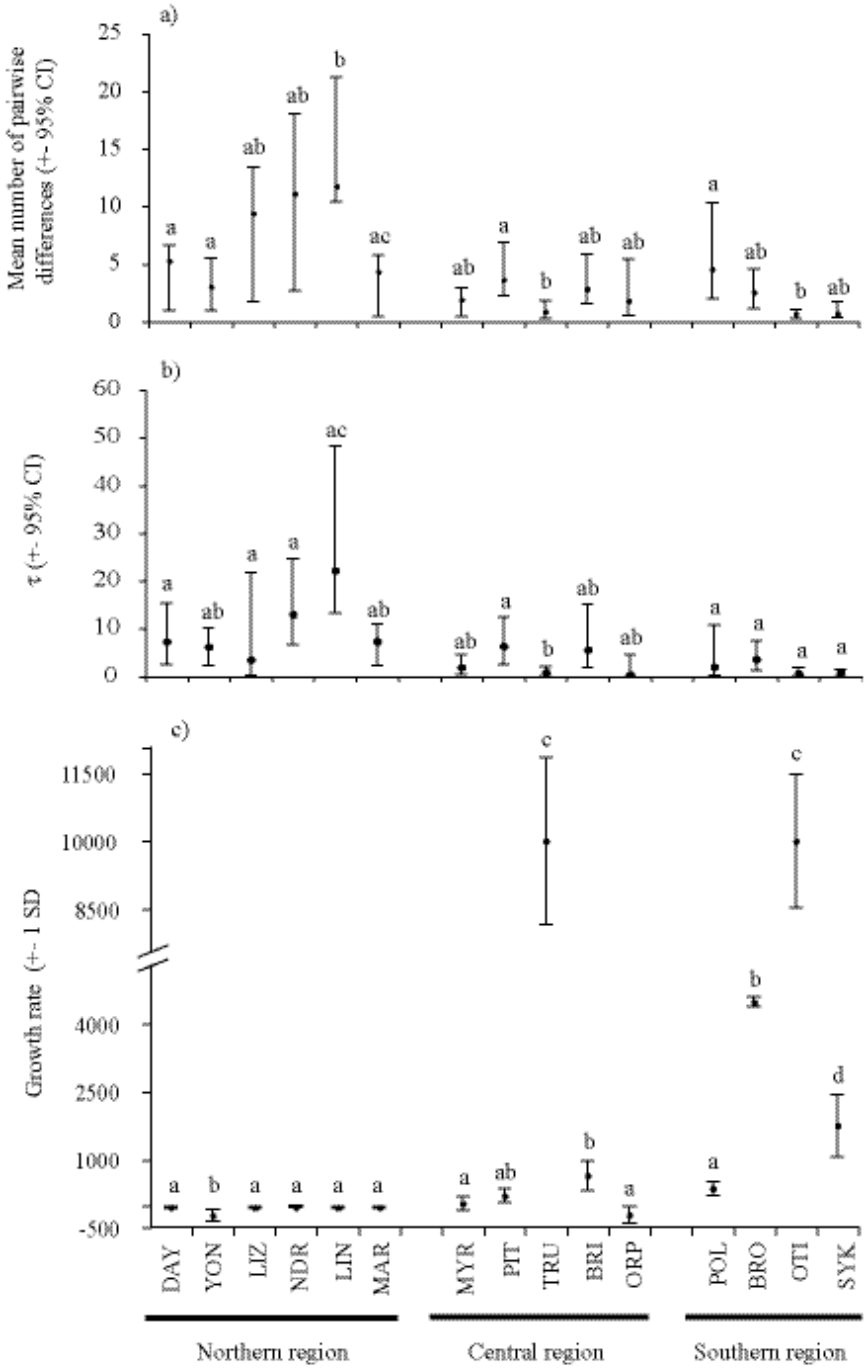

Fig. 6: Mismatch means, expansion parameter (τ) and growth rate (*g*) among reefs within regions. Location abbreviations follow Fig. 4. Statistical differences have been indicated for each region separately with letters (shared letter = not significantly different).

Table 2: Results of the demographic bottleneck analyses: mismatch means (mismatch), sums of squared deviations (SDD), probability (p) of sudden expansion, sequential Bonferroni corrected significance level (α), one-tailed probabilities of heterozygotic excess using a Wilcoxon test under the Infinite Allele Model (IAM) and the stepwise mutation Model (SMM).

	MtDNA				Microsatellites	
Region, clade or reef	Mismatch	SDD	p	α	IAM	SMM
NORTH	12.293	0.045	0.02ns	0.003	0.125 ns	1.00 ns
CENTRAL	3.939	0.007	0.33 ns	0.005	0.934 ns	0.938 ns
SOUTH	2.373	0.004	0.61 ns	0.01	0.813 ns	1.00 ns
Clade 2	2.801	0.055	0.22 ns	0.004		
Clade 3	5.618	0.002	0.64 ns	0.01		
Clade 3N	3.576	0.006	0.45 ns	0.006		
Day Reef	5.273	0.051	0.35 ns	0.005	0.063 ns	1.00 ns
Yonge Reef	3.032	0.198	0.01 ns	0.003	0.188 ns	0.938 ns
Lizard Island	9.395	0.050	0.24 ns	0.004	0.813 ns	0.938 ns
North Direction	11.11	0.140	0.000 *	0.002	0.125 ns	0.938 ns
Linnet Reef	11.76	0.097	0.000 *	0.003	0.063 ns	0.938 ns
Martin Reef	4.343	0.032	0.58 ns	0.007	0.063 ns	0.938 ns
Myrmidon Reef	1.919	0.017	0.39 ns	0.006	0.813 ns	1.000 ns
Pith Reef	3.619	0.074	0.03 ns	0.003	0.938 ns	1.000 ns
Trunk Reef	0.857	0.001	0.81 ns	0.03	0.938 ns	1.000 ns
Britomart Reef	2.830	0.051	0.16 ns	0.003	0.063 ns	0.875 ns
Orpheus Island	1.819	0.012	0.58 ns	0.008	0.813 ns	1.000 ns
Polmaise Reef	4.551	0.011	0.73 ns	0.02	0.875 ns	0.938 ns
Broomefield Reef	2.561	0.006	0.83 ns	0.05	0.125 ns	0.938 ns
One Tree Island	0.705	0.007	0.28 ns	0.004	0.813 ns	1.000 ns
Sykes Reef	0.692	0.0321	0.01 ns	0.003	0.813 ns	1.000 ns

Statistical significance: * = $p < 0.0001$, ns = not significant.

The lower genetic diversities in the southern region identified here agrees with previous reports (e.g., Doherty et al. 1994; van Herwerden and Doherty 2006). However, the mean number of pairwise differences and the expansion parameter (τ) for the southern region identified here were not significantly different to estimates obtained from the central and northern regions. This contrasts with a previous report (van Herwerden and Doherty 2006) that the southern region had undergone a more ancient population expansion based on the mean number of pairwise differences and the expansion parameter (τ). The 95% confidence interval of their estimates, however, overlapped among regions indicating that they were not significantly different. I suggest that the southern region has undergone a more recent population expansion compared to the other two regions. This interpretation is based on the results of both the mismatch analysis (the lower bound of the 95% confidence interval of τ could not be distinguished from 0 in the southern region) and the population expansion analysis (population expansion rate was significantly greater in the southern region). These results support the predictions that local extinctions may affect the metapopulation dynamics towards the species margin to a greater extent than within more centrally located regions (Lennon et al. 1997; Holt and Keitt 2000).

Population Demography among Locations

There were substantial differences in the genetic diversities, mismatch means and population growth rates among reefs within regions (Fig. 4 and 6). Four general patterns were observed (Table 3). The majority of populations conformed to a model of mutation-drift equilibrium with no evidence of local extinctions. In contrast, two populations in the northern region (North Direction, Linnet) conformed to a model of migration-drift equilibrium with a departure from panmixia (Table 3). Very high nucleotide diversities in these locations (Fig. 4b, Fig. 6a) argue against a model of sudden expansion (Table 2). These high diversities were most likely the result of the presence of approximately equal numbers of individuals from two differentiated lineages at these locations (Fig. 2). Because the sudden expansion model was supported in both these lineages when analysed independently (Clade 2 and Clade 3N Table 2), it is likely that these differences were caused by a departure from panmixia, rather than long-term stability of the populations leading to the accumulation of diversity via mutation.

Such sub-structure within populations violates the assumption of mismatch analysis of panmixia (Slatkin and Hudson 1991) and this result highlights the potential role of departures from the assumptions of demographic history analyses (Knowles and Maddison 2002; Knowles 2004).

Only a single reef (i.e., Yonge) provided support for a model of a weak bottleneck or a large bottleneck followed by migrant-pool colonisation, where colonisers originate from many sources (Wade and McCauley 1988; McCauley 1991) (Table 3). Genetic diversity estimates were significantly lower at this reef than other northern reefs (Fig. 4a – c) but this low diversity was not associated with a higher population expansion rate (Fig. 6c). The genetic pattern observed at this reef may be expected if a local population reduction was followed by a migrant-pool colonisation event. If colonisers were few, but from a range of genetically differentiated populations, this could lead to reduced genetic diversities, but not necessarily a shorter coalescent history (Pannell and Charlesworth 2000; Pannell 2003). Conversely, it is possible that the observed reduction here in local genetic diversity (π_S) was not great enough to result in a bottleneck (Nei et al. 1975) although a large genetic bottleneck, identified by a high expansion rate, was detected in the population from Trunk Reef which displayed a similar reduction in local genetic diversity (π_S).

Populations on three reefs, Trunk, One Tree Island and Sykes, conformed to a model of a large bottleneck and/or extinction followed by propagule-pool colonisation, where colonisers originate from a single source (Wade and McCauley 1988; McCauley 1991) (Table 3). These locations were characterised by low local diversity (π_S) and high population expansion rates. In addition, the expansion parameter (τ) for these populations did not differ from 0 (Fig. 6b) and, therefore, their expansion times could not be distinguished from the present. In concert, these results provide strong evidence for recent population bottlenecks and/or local extinctions in these populations with re-colonisation most likely following the propagule-pool model. This finding suggests that the evolution of marine metapopulations may be more greatly affected by local extinctions than previously thought (Planes et al. 1996; Planes 2002). The southern region was characterised by a high frequency of local populations with reduced genetic diversity (π_S), which resulted in a reduction of regional diversity (π_T) for that region. Therefore, there appears to be considerable potential for local genetic bottlenecks and/or

extinctions to affect regional genetic diversity (π_T), and consequently, the evolutionary potential and the metapopulation dynamics of this marine species.

Table 3: Models of the demographic histories of populations of *Acanthochromis polyacanthus* on the Great Barrier Reef and criteria including genetic diversity (π_S), conformation to the sudden expansion model and population growth used to assess support for each model.

Model of demographic history	π_S	Sudden expansion	Population growth	Examples
Migration-drift equilibrium	High	Retained	Low	DAY, MYR
Migration-drift equilibrium and departure from panmixia	High	Rejected	Low	NDR, LIN
Small population size reduction or extinction and migrant-pool colonisation	Low	Retained	Low	YON
Large population reduction and/or extinction and propagule-pool colonisation	Low	Retained	High	TRU, OTI, SYK

Nuclear vs. mtDNA Diversity and Historical Demography Analyses

Patterns of microsatellite allelic diversity largely matched those recorded by the mtDNA except among populations in the southern region (Fig. 3 and 4). In this region, there was an opposing pattern where locations displayed high mtDNA diversity associated with low allelic diversity and vice versa (Fig. 4a and c). It is possible that these discrepancies can, in part, be explained by variations in sample sizes given the sensitivity of allelic diversity estimates to sample size (Leberg 2002). Indeed, the population here with the lowest allelic diversity was also the population with the smallest sample size (18 alleles). In contrast, however, allelic diversities were significantly different between Broomefield and One Tree Island despite similar sample sizes (34 and 36). Therefore, differences in sample sizes are unlikely to be the only source of variation in the allelic diversity estimates reported here.

None of the regions, or populations within regions, were characterised by heterozygote excess, regardless of the model of microsatellite evolution used (Table 2). The absence of a bottleneck signal in the nuclear markers may be a result of differences

in the effective population sizes of nucDNA and mtDNA (Avise 2000). Because of the four-fold difference in effective population size a smaller population reduction may result in a bottleneck in the mtDNA but not in the nucDNA. Furthermore, if present, the genetic signal of demographic bottlenecks may be rapidly erased in nuclear markers (Cornuet and Luikart 1996). It is, however, also possible that the genetic bottlenecks observed in some of populations examined here were restricted to the mitochondrial genome. For example, a selective sweep on functional mtDNA genes, physically linked to the Control region (Rand 2001), could result in a similar pattern but without the severe reduction in population size characteristic of a bottleneck. It is also possible, that the number of loci used in this study was insufficient to detect bottlenecks that were indeed present. Concomitant reductions in allelic and mtDNA diversities found in some populations (e.g., Yonge and Trunk Fig. 4a – c) suggest that the bottlenecks indicated by the control region data were not restricted to the mitochondrial genome. Instead, the absence of genetic bottlenecks in the microsatellites are likely to have been caused by the number of microsatellite loci used here, the greater effective population size and the slower fixation of nuclear genes.

Phylogenetic Structure and Species Status

The phylogenetic analysis presented here resolved four highly divergent lineages of *A. polyacanthus* in the set of sampled populations. Two of these lineages consisted exclusively of the bicoloured morph in the northern region of the GBR (Fig. 2). The two lineages of bicoloured morphs co-occurred on a large proportion of sampled reefs in the northern region and the frequency of Clade 2 individuals increased across the continental shelf toward the west. According to our analyses, Clade 1 (black southern fish) and Clade 2 (northern bicoloured fish) were more closely related to each other than were Clade 2 and Clade 3 (northern and central bicoloured fish) and Clade 3 and Clade 4 (Melanesian bicoloured fish). This contrasts with the findings of van Herwerden and Doherty (2006) who reported monophyly among all northern fish and Planes et al. (2001) who reported chromatic monophyly. Differences between this study and the previous ones may have resulted from the inclusion of both transitions and transversions in the current phylogeny. The sequences used here showed a low ts/tv ratio, indicating that transitions carried significant information, and that combined with the lack of compositional heterogeneity between sequences indicated that using all substitution types was appropriate for these data.

Previous authors (e.g., Planes et al. 2001; van Herwerden and Doherty 2006) have argued that the depth of genetic divergence between the southern black and the northern bicoloured morphs warrants species status and have recommended a taxonomic review of *Acanthochromis*. The sequence divergences between black (Clade 1) and bicoloured morphs (Clade 2) found here, however, appeared to be less than the divergence among geographically disjunct bicoloured populations Clade 2 or 3 vs. Clade 4). I also found deep sequence divergence between bicoloured individuals co-existing on the same reefs (Clade 2 and 3). I propose, therefore, that the considerable genetic structure of chromatically similar and geographically co-occurring individuals does not support the simple interpretation of two species congruent with colour morph. The presence and maintenance of two or more divergent lineages within populations across relatively small spatial scales is emerging as a feature of many coral reef organisms (e.g., Knowlton 1993; Barber et al. 2000; Bernardi et al. 2003; Bay et al. unpublished data). Exactly how many divergent lineages of *A. polyacanthus* co-occur on the GBR, and whether the degree of divergence that is present constitutes species status will require further study. In the meantime, however, the data presented here do not support a single division of what is currently recognized as *A. polyacanthus* into two species aligned with colour morphs.

Conclusion

The variation in genetic diversities and population expansion rates among populations reported here strongly indicate that *A. polyacanthus* functions as a metapopulation and that local extinctions may play an important part in the evolutionary dynamics of this species through founder effects. These conclusions contrast with previous suggestions that genetic bottlenecks and/or local extinctions are unimportant in the metapopulation dynamics of coral reef fishes. The development and application of highly sensitive molecular markers and within-region sampling have the potential to illuminate the presence of metapopulations and the role of local extinctions in marine species with higher gene flow.